Available online at www.sciencedirect.com
ScienceDirect
Journal of Environmental Sciences 2010, 22(4) 486–493
JOURNAL OF ENVIRONMENTAL SCIENCES
ISSN 1001-0742
CN 11-2629/X
www.jesc.ac.cn

Enhanced adsorption of Methylene Blue from aqueous solution by chitosan-*g*-poly (acrylic acid)/vermiculite hydrogel composites

Yi Liu[1,2], Yian Zheng[1], Aiqin Wang[1,*]

1. Center of Eco-material and Green Chemistry, Lanzhou Institute of Chemical Physics, Chinese Academy of Sciences, Lanzhou 730000, China. E-mail: liuyiyongcheng@163.com
2. Graduate University of the Chinese Academy of Sciences, Beijing 100049, China

Received 29 June 2009; accepted 01 September 2009; accepted 04 September 2009

Abstract

A series of chitosan-*g*-poly (acrylic acid)/vermiculite hydrogel composites were synthesized and used as adsorbents for the investigation of the effect of process parameters such as vermiculite content, pH of dye solution, contact time, initial concentration of dye solution, temperature, ionic strength and concentration of surfactant sodium dodecyl sulfate on the removal of Methylene Blue (MB) from aqueous solution. The results showed that the adsorption capacity for dye increased with increasing pH, contact time and initial dye concentration, but decreased with increasing temperature, ionic strength and sodium dodecyl sulfate concentration in the present of the surfactant. The adsorption kinetics of MB onto the hydrogel composite followed pseudo second-order kinetics and the adsorption equilibrium data obeyed Langmuir isotherm. By introducing 10 wt.% vermiculite into chitosan-*g*-poly (acrylic acid) polymeric network, the obtaining hydrogel composite showed the highest adsorption capacity for MB, and then could be regarded as a potential adsorbent for cationic dye removal in a wastewater treatment process.

Key words: hydrogel composites; vermiculite; Methylene Blue; adsorption kinetics; adsorption isotherms
DOI: 10.1016/S1001-0742(09)60134-0

Introduction

A very small amount of dye in water is highly visible. Discharging even a small amount of dye into water can affect aquatic life and food webs due to the carcinogenic and mutagenic effects of synthetic dyes. Therefore, the removal of dyes from waste effluents is always widely focused (Robinson et al., 2001; Crini and Badot, 2008). Techniques such as coagulation, chemical precipitation, membrane filtration, solvent extraction, reverse osmosis and adsorption have been used in wastewater treatment. Among them, adsorption is recognized as a promising technique due to its ease of operation, easy availability, simplicity of design, high efficiency, comparable low cost of application in decoloration process and ability to treat dyes in more concentrated forms (Meshko et al., 2001; Sanghi and Bhattacharya, 2002).

The most widely used adsorbent is commercial activated carbon, but the cost and the difficulty of regeneration limit its application (Özcan and Özcan, 2004). For this reason, many researchers divert to low cost, economic and effective substitutes, like wheat shells (Bulut and Aydın, 2006), immobilized laccase (Wang et al., 2008b), coconut husk (Tan et al., 2008), spent tea leaves (Hameed, 2009), fly ash (Janoš et al., 2003), surface soils (Qu et al., 2008) and sand (Bukallah et al., 2007). Clays have gained increasing interest because of their low cost, abundance and potential for ion exchange. Therefore, several raw clays and their ramifications were used to remove dyes, such as sepiolite (Eren and Afsin, 2007), kaolin (Nandi et al., 2009), montmorillonite (Wang and Wang, 2007), bentonite (Bulut et al., 2008) and silica nano-sheets derived from vermiculite (Zhao et al., 2008). However, some of these adsorbents do not have good adsorption capacities for the dyes. Hence, there is a need to search for more effective adsorbents.

Recently, the polymer/clay hydrogel composite has received great attention because of its relatively low production cost and high adsorption capacity for some dyes (Wang et al., 2008a). Hydrogel is a porous three-dimensional polymeric network, and its special structure allows the diffusion of solutes into the interior network. Also, hydrogel is in possession of lots of ionic or nonionic functional groups, which can absorb or trap ionic dyes from wastewater (Paulino et al., 2006). Vermiculite (VMT) is a layered aluminum silicate with exchangeable cations and active –OH groups on the surface. However, to the best of our knowledge, little information has been reported with regard to the adsorption of Methylene Blue (MB) by polymer/VMT hydrogel composite. Based on the merits of VMT and hydrogels composite, a series of chitosan-*g*-poly

* Corresponding author. E-mail: aqwang@lzb.ac.cn

(acrylic acid)/vermiculite (CTS-*g*-PAA/VMT) hydrogel composites were synthesized and used as adsorbents to remove MB from aqueous solution in this study. The effects of various experimental parameters such as VMT content, pH of dye solution, contact time, initial concentration of dye solution, temperature, ionic strength and concentration of sodium dodecyl sulfate (SDS) on the adsorption process were evaluated. In addition, the equilibrium isotherms and the adsorption kinetics of MB onto the composite were investigated systematically.

1 Materials and methods

1.1 Materials and chemicals

Acrylic acid (AA, chemically pure) was distilled before use. The initiator, ammonium persulfate (APS, analytical grade) was recrystallized from distilled water before use and the crosslinker, *N,N*'-methylenebisacrylamide (MBA, chemically pure) was used without further purification. AA, APS and MBA were purchased from Shanghai Reagent Corp. (China). Chitosan (CTS) with the deacetylation degree of 0.90 and viscosity-average molecular weight of 3.0×10^5 was obtained from Zhejiang Yuhuan Ocean Biology Co. (China). Vermiculite (Gansu Xinyi Environmental Protection Technology Co., Ltd., China) was milled through a 320-mesh screen. VMT micropowder was calcined at 500°C and then cooled to room temperature in a desiccator for further studies. Sodium dodecyl sulfate (SDS, chemically pure) was purchased from Beijing Donghuan Joint Chemical Products Factory (China). Methylene Blue was purchased from Alfa Aesar A Johnson Matthey Company (UK) and used as received. Other reagents used were all of analytical grade and all solutions were prepared with distilled water.

1.2 Preparation of CTS-*g*-PAA/VMT hydrogel composites

CTS-*g*-PAA/VMT was prepared according to our previous report (Xie and Wang, 2009). Briefly, 0.5 g CTS was dissolved into 30 mL acetic acid solution (1%) in a 250-mL four-neck flask, equipped with a mechanical stirrer, a reflux condenser, a funnel and a nitrogen line. APS 0.10 g was added into the flask to initiate CTS to produce radicals after being purged with nitrogen for 30 min to remove oxygen dissolved in the system. Ten minutes later, the mixture of 3.60 g AA, 0.25 g MBA, different amounts of VMT and 10 mL water was added. The water bath was kept at 70°C for 3 hr to accomplish the reaction, then the resulting product was washed with distilled water to remove residual reactants and shifted into 1 mol/L NaOH solution to neutralize pH to 7 until swelling equilibrium was achieved and then dehydrated with industrial ethanol. The sample was dried to a constant weight at 70°C, and then the product was milled through a 200-mesh screen and used for further experiments. CTS-*g*-PAA hydrogel was prepared according to a similar procedure except without VMT.

1.3 Adsorption studies

Adsorption experiments were carried out on thermostated shaker (THZ-98A) at a constant speed of 120 r/min with 50 mL MB solution of known concentration and pH, and 0.025 g adsorbent was added into a 100-mL stoppered conical flask. To study the effect of the amount of VMT, pH of MB solution, contact time, initial MB concentration solution temperature, ionic strength and SDS concentration on the adsorptive removal of MB, batch experiments were conducted. Effect of VMT content was investigated with a series of adsorbent and dye solution (pH = 7) mixture in each flask for 240 min. Then optimum adsorbent was chosen for the following experiments. Effect of pH on dye removal was studied over a pH range 2–9 and the dye pH was adjusted with dilute aqueous solution of NaOH or HCl (0.1 mol/L). Effect of adsorptive time on dye removal was conducted at pH 7 for predetermined time intervals. For isotherm studies, a series of flasks with MB solution in the range of 700–1200 mg/L at pH 7 was prepared and then the adsorbent was added to each flask. The mixtures were agitated at constant temperature of 30, 40 and 50°C for 240 min. Effect of ionic strength on dye removal was determined by mixing 50 mL MB solution at natural pH (4.7) with 0.025 g adsorbent with the addition of different amounts of sodium chloride for 90 min. Effect of SDS concentration on adsorption of MB was investigated under the same conditions except for the addition of different concentrations of SDS rather than sodium chloride. The suspension was centrifuged at 5000 r/min for 10 min and the absorbance of the supernatant was measured. The concentration of residual color of MB in the adsorption media was measured by a UV-Vis spectrophotometer (Specord 200, Analytic Jena, Germany) at a wavelength corresponding to the maximum absorbance, about 670 nm for MB. Calibration curve was plotted between absorbance and concentration of MB solution.

The adsorption capacity was calculated by the following Eq. (1):

$$q = \frac{(C_i - C_f) \times V}{W \times 1000} \tag{1}$$

where, q (mg/g) represents the amount of MB adsorbed onto adsorbent; C_i and C_f (mg/L) represent MB concentration before and after adsorption, respectively; V (mL) is MB solution volume used and W (g) is the weight of adsorbent.

1.4 Characterization

Infrared spectra of the samples were obtained using a Fourier transform infrared spectroscopy (FT-IR) spectrophotometer (NEXUS, Thermo Nicolet, USA) in the wavenumber range of 4000–400 cm^{-1} using KBr pellet.

2 Results and discussion

2.1 FT-IR spectra of adsorbents

The infrared spectra of CTS-*g*-PAA/10% VMT, CTS-*g*-PAA and 500°C calcined VMT are shown in Fig. 1. The

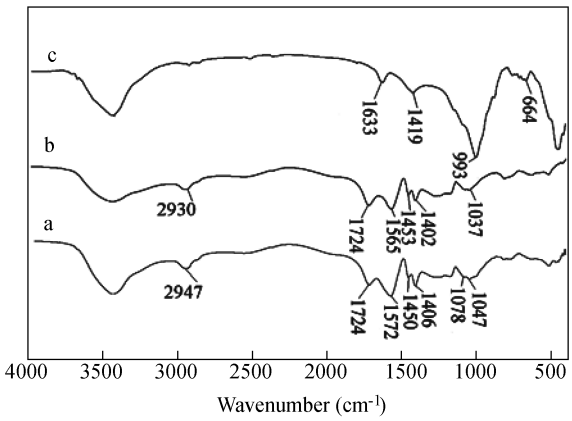

Fig. 1 Spectra of CTS-*g*-PAA/10% vermiculite (VMT) (a), CTS-*g*-PAA (b) and 500°C calcined VMT (c).

characteristic bands at 1724, 1565, and 1402 cm^{-1} (Fig. 1b) are assigned to –C═O stretching of –COOH, $–COO^-$ asymmetric stretching, and $–COO^-$ symmetric stretching, respectively. The characteristic absorption bands of N–H and C_3–OH of CTS could not be found, indicating that $–NH_2$, –NHCO and –OH of CTS participated in graft reaction with AA (Xie and Wang, 2009). Compared with infrared spectra of calcined VMT and CTS-*g*-PAA, the infrared spectrum of composite containing 10 wt.% VMT showed a broad band in 3700–3300 cm^{-1}, which is characteristic absorption band of water molecule. The bands of $–COO^-$ asymmetric stretching and $–COO^-$ symmetric stretching were shifted. However, the bands at about 993 cm^{-1} and 664 cm^{-1} corresponding to stretching vibrations of Si–O bond (Tomanec et al., 1997) almost disappeared in the spectrum of composite, indicating the reactions between $–COO^-$ groups and –OH groups on the surface of VMT.

2.2 Effect of vermiculite content

As shown in Fig. 2, it is clear that VMT content plays an important role on adsorption capacity of the adsorbent for MB. It increased from 1571.26 to 1612.32 mg/g for CTS-*g*-PAA/VMT as 10 wt.% VMT was introduced. However, the adsorption capacity decreased with further increasing VMT content and the adsorption capacity for MB was only 16.75 mg/g using VMT as the adsorbent, indicating that an appropriate introduction of VMT into the pure polymer can improve the adsorption capacity. The result may be attributed to that at low VMT content (10 wt.%), VMT is easily ionized and dispersed into CTS-*g*-PAA gels, thus enhancing the hydrophilicity of the hydrogel which is favor for the adsorption of MB (Lee and Yang, 2004). At higher VMT content, above 10 wt.%, more VMT particles act as an additional network point, then the reaction occurs between –OH groups on the surface of VMT and $–COO^-$ groups, and accordingly, the crosslink density of the hydrogel becomes larger. In addition, the amount of ionic groups like $–COO^-$ groups decreases, which is also an important reason for the decrease in the adsorption capacity for MB (Lin et al., 2001; Li et al., 2004). As a consequence, CTS-*g*-PAA/10% VMT was used in further studies.

2.3 Effect of pH

The pH of dye solution is a very important factor for the dye removal, which can change the surface charge of an adsorbent, and at the same time, can promote or depress the ionization of adsorbent and dye (Qada et al., 2006). The pH of dye solution may also change the molecular structure of dye, and therefore the removal of ionic dye can be influenced greatly. Figure 3 shows that the adsorption capacity of the adsorbent had a sharp increase with increasing initial pH values, but when the pH increased up to 7, the adsorbed amount of MB almost kept constant. Similar phenomena were reported by many researchers (Bhattacharyya and Sharma, 2005; Wang et al., 2008a; Cengiz and Cavas, 2008). Furthermore, the final pH of MB solution after adsorption tended to 6 after the initial pH reached 4. The results may be attributed to the following factors. At lower pH values, hydrogen ion competes with MB cation, and most of the carboxyl of adsorbent exist in the form of –COOH, which reduce the adsorbed amounts for MB. At higher pH values, more hydroxyls and $–COO^-$ occur, which may enhance electrostatic attraction and the adsorption capacity of adsorbent for MB. Then further studies were carried out with pH 7 of dye solution.

2.4 Effect of contact time

Figure 4 shows adsorption capacities versus contact time at 30°C. The adsorption capacity of the hydrogel composite for MB increases rapidly within 60 min, then changes slightly until 90 min, after that no further adsorption occurs with prolonged time. Consequently, the equilibrium time

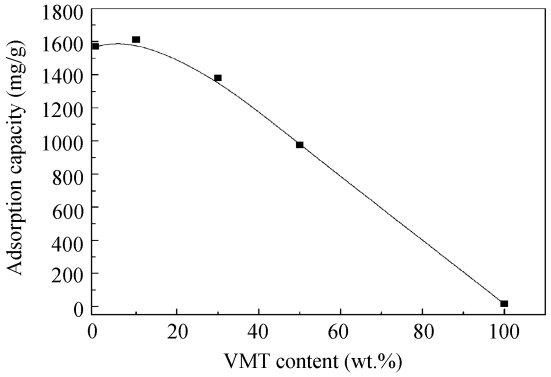

Fig. 2 Effect of VMT content on Methylene Blue (MB) adsorption.

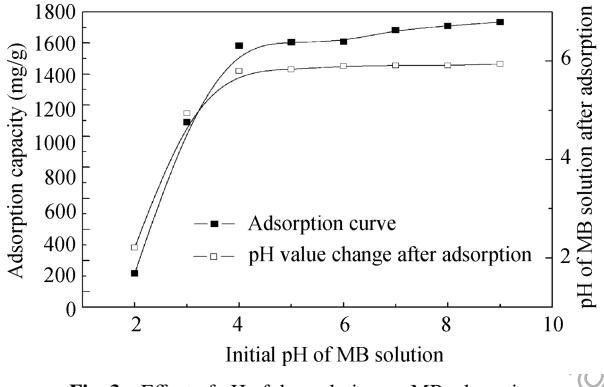

Fig. 3 Effect of pH of dye solution on MB adsorption.

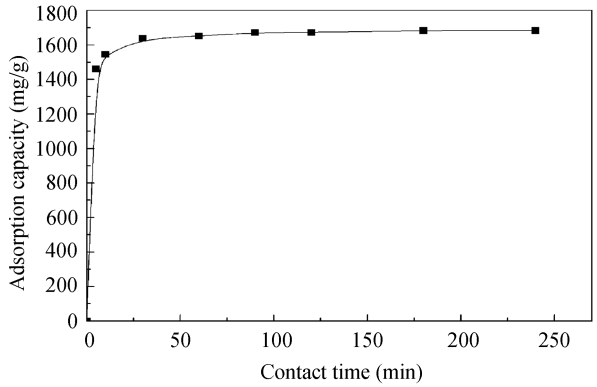

Fig. 4 Effect of contact time on MB adsorption.

is 90 min in our experiment for the adsorption of MB onto as-prepared adsorbent. Time-rate adsorption curve is single and continuous, suggesting the possibility of monolayer coverage of MB onto the surface of adsorbent (Senthilkumaar et al., 2005).

2.5 Effect of initial concentration and solution temperature

To determine the influence of initial MB concentration and solution temperature on the equilibrium uptake, the initial MB concentration varied from 700 to 1200 mg/L at 30, 40 and 50°C, as illustrated in Fig. 5. It showed that the initial concentration of dye solution affect the adsorption capacity greatly. The adsorption capacity increased sharply until the concentration of dye solution increased up to 1000 mg/L, thereafter reaching a plateau for adsorbent at different temperatures, indicating that dye removal was highly dependent on initial dye concentration. The larger removal amount of MB caused by a higher initial MB concentration was presumably attributed to the active interaction between adsorbent and dye molecules. The findings probably were also due to that an increase in dye concentration could accelerate the diffusion of dye molecules onto the adsorbent as a result of an increase in the driving force of concentration gradient (Özer and Dursun, 2007). With the progress of adsorption, the availability of adsorption sites of the adsorbent got diminished, leading the adsorption capacity to be constant. In addition, it is observed that the adsorption capacity of adsorbent for MB decreased as increasing temperature. The result may be attributed to that changing temperature could change the equilibrium capacity of the adsorbent for a particular adsorbate (Qodah, 2000; Doğan et al., 2004).

2.6 Effect of ionic strength

The removal of dyes depends greatly on electrostatic parameters such as surface charge, pH and ionic strength (Aguedach et al., 2008). Ionic strength plays a major role in the electrical double layer (EDL) structure of a hydrated particle. The thickness of the DEL decreases as the ionic strength increasing, resulting in a decrease in adsorption (Weng and Pan, 2006). In this work, the effect of the additional amounts of NaCl was studied at the natural pH of MB (4.7). It can be seen from Fig. 6 that the adsorption capacities decreased with increasing NaCl concentration for the adsorbent. The result is consistent with that of Weng and Pan (2006). The ionic strength increases as NaCl concentration increases and more Na^+ ions can screen the negative sites of the adsorbent, leading to the reduce of electrostatic attractive force, and accordingly, the amount adsorbed for MB decreases (Aguedach et al., 2008). Ghasemi and Asadpour (2007) pointed out that the ionic strength may also lead to the dimerisation process of MB molecules, thereby reducing electrostatic force in the presence of high concentration of Na^+ and Cl^- ions.

2.7 Effect of SDS concentration

Surfactants, especially the anionic surfactants, are used in huge amounts in industries and discharged into wastewater, and thus bring adverse influence. As a consequence, the effect of the anionic surfactant SDS on MB removal was examined in the present work. It can be seen from Fig. 7 that the adsorption capacity of the adsorbent for MB decreased with increasing SDS concentration and the presence of SDS could enhance the MB adsorption capacity. Even when the concentration of SDS was as high as 0.12 wt.%, the adsorption capacity could reach 1573.87 mg/g, while the adsorption capacity was 1565.71 mg/g without the SDS. This phenomenon possibly attributed to the following factors. At lower surfactant concentrations, surfactant may be adsorbed onto adsorbent which increased the affinity for dyes leading to an increasing removal amount of dyes. As surfactant concentration increasing, surfactant may form micelles which can dissolve dyes thus

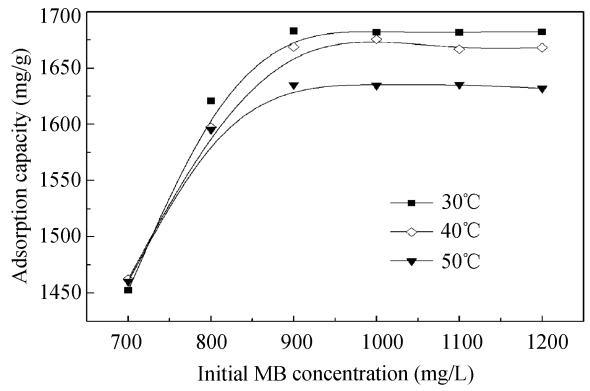

Fig. 5 Effect of initial MB concentration and solution temperature on MB adsorption.

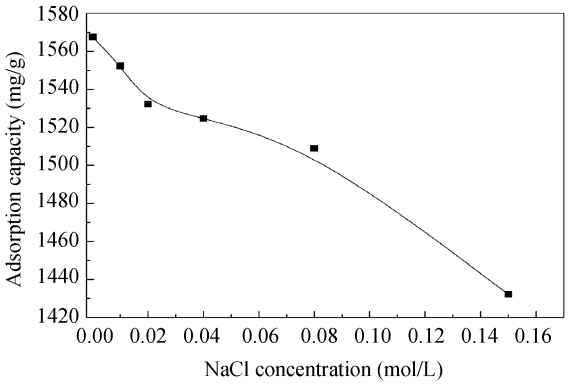

Fig. 6 Influence of ionic strength on the removal amount of MB on adsorbent.

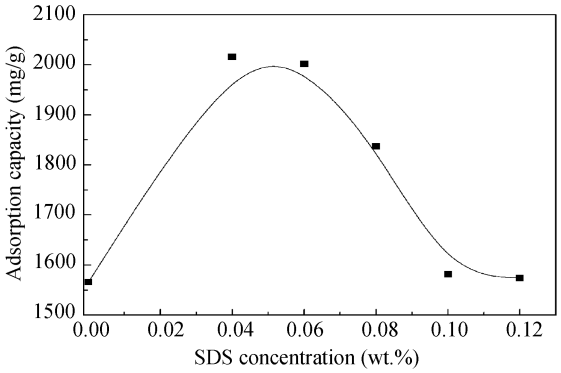

Fig. 7 Effect of SDS concentration on MB removal.

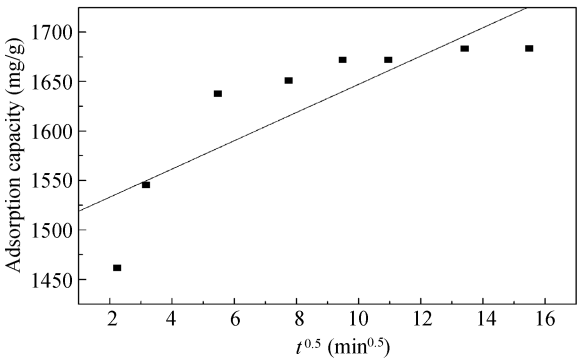

Fig. 8 Intra-particle diffusion plot for MB on adsorbent.

hamper the dye adsorbed onto adsorbent, and lead to the reduction of amount of dye onto adsorbent (Janoš and Šmídová, 2005). This result is interesting and suggests that a limited SDS is favorable for the dye removal. Similar result has also been reported by Barhoumi et al. (2003).

2.8 Adsorption kinetics

In order to understand the process of adsorption, three kinetic models were applied to analyze experimental data.

The linear form of pseudo first-order kinetic model of Lagergren is expressed as Eq. (2) (Lagergren and Svenska, 1898)

$$\log(q_{1e}-q_t) = \log q_{1e} - K_1 t/2.303 \quad (2)$$

where, q_{1e} and q_t represent the amount of dye adsorbed on adsorbent at equilibrium and any time, respectively, and K_1 (min^{-1}) is rate constant. q_{1e} and K_1 can be obtained by the intercept and slope of plot of $\log(q_{1e}- q_t)$ against t.

The linear form of Ho's pseudo second-order kinetics, is shown as Eq. (3) (Ho and Mckay, 1998)

$$t/q_t = 1/(K_2 q_{2e}^2) + t/q_{2e} \quad (3)$$

where, q_{2e} and q_t represent the same meanings as those of pseudo first-order model, and K_2 (g/(mg·min)) is the pseudo second-order rate constant. q_{2e} and K_2 can be calculated from the slope and intercept of plot t/q_t versus t.

Intra-particle diffusion model is an empirical found functional relationship, assuming that the adsorption capacity varies almost proportionally with $t^{0.5}$ (Weber and Morris, 1962) (Eq. (4)):

$$q_t = K_{id} t^{0.5} + C \quad (4)$$

where, K_{id} (mg/(g·min$^{1/2}$)) is the intra-particle diffusion rate parameter. According to the equation, a plot of q_t versus $t^{0.5}$ should be a straight line with a slope K_{id} and intercept C when the adsorption mechanism follows intra-particle diffusion process. The value of C indicates the thickness of boundary layer, and with the larger value of C the contribution of the surface sorption is greater in the rate limiting step (Kannan and Sundaram, 2001). It can be seen from Fig. 8 that the sorption process tended to follow two distinct phases.

In this study, the three models were tested for MB on CTS-*g*-PAA/10% VMT. The best-fit model was determined depending on the linear correlation coefficient R^2. The results are shown in Table 1. The correlation coefficient of pseudo second-order which was close to unit was much higher than that of pseudo first-order and the theoretical q_{2e} value computed from pseudo second-order was much closed to the experimental q_{exp} value given in Table 1, indicating that the pseudo second-order model was more applicable for the system, while theoretical q_{1e} value estimated from pseudo first-order kinetic did not give reasonable value, suggesting this model could not be used to depict the adsorption data of MB onto the adsorbent.

2.9 Adsorption isotherm

For the purpose of adsorption system design, adsorption isotherms, depicting how adsorbed molecule interacts with adsorbent, are commonly used to analyze equilibrium data. The analysis of the isotherm data is of great importance by fitting them to different isotherm models to optimize the adsorption system. The most widely used isotherm equations are Langmuir and Freundlich equations.

Langmuir isotherm is based on the assumption that an activate point on the surface of the adsorbent is able to adsorb one molecule, indicating the adsorbed layer is one molecule thick. It is expressed as the following Eq. (5):

$$C_{eq}/q_{eq} = 1/(b \times q_m) + C_{eq}/q_m \quad (5)$$

where, C_{eq} (mg/L) is the equilibrium concentration, q_{eq} (mg/g) is the amount adsorbed, q_m (mg/g) is complete monolayer adsorption capacity, and b (L/mg) is the Langmuir constant. The dimensionless separation factor, R_L, is essential characteristic of Langmuir isotherm, which is

Table 1 Kinetic parameters of three models for MB onto adsorbent

Adsorbent	CTS-*g*-PAA/10% VMT	
Pseudo first-order	K_1 (min^{-1})	0.0370
	R^2	0.8903
	q_{1e} (mg/g)	365.65
	q_{exp} (mg/g)	1683.70
Pseudo second-order	q_{2e} (mg/g)	1690.64
	K_2 (g/(mg·min))	5.75×10^{-4}
	R^2	1
Intra-particle diffusion	K_{id} (mg/(g·min$^{1/2}$))	14.27
	C	1504.61
	R^2	0.7115

defined as Eq. (6) (Hall et al., 1966):

$$R_L = 1/(1+bC_0) \quad (6)$$

where, b is the Langmuir constant and C_0 is the highest initial MB concentration. The value of R_L indicates the type of the isotherm to be either favorable ($0 < R_L < 1$), unfavorable ($R_L > 1$), linear ($R_L = 1$) or irreversible ($R_L = 0$) (Hall et al., 1966).

Freundlich isotherm is valid for non-ideal adsorption on heterogeneous surfaces, suggesting multilayer adsorption on adsorbent surfaces. The empirical equation is presented as following Eq. (7):

$$\log q_{eq} = \log K_F + \frac{1}{n} \times \log C_{eq} \quad (7)$$

where, K_F ((mg/g)(L/mg)$^{1/n}$) is the Freundlich adsorption constant and the slope of the Freundlich equation $1/n$ ranging between 0 and 1 is a measure of adsorption intensity or surface heterogeneity, which may become more heterogeneous when $1/n$ gets close to zero (Haghseresht and Lu, 1998). The value of $1/n$ below one suggests a normal Langmuir isotherm while $1/n$ above one is indicative of cooperative adsorption (Fytianos et al., 2000).

Langmuir and Freundlich isotherms for the studied system at different temperatures are presented in Fig. 9a, b, respectively, and the Langmuir and Freundlich parameters computed from Eq. (5)–(7) are listed in Table 2. The best-fit isotherm model for the system was compared by judging the correlation coefficients, R^2 values. It can be seen from Table 2, the Langmuir model showed the best fit with the highest R^2 values at all temperatures compared to Freundlich model for the adsorbent, suggesting homogeneous surfaces of adsorbent and monolayer coverage of MB onto the adsorbent. This finding is consistent with the conclusion obtained from the effect of contact time on adsorption capacity. The values of R_L at all temperatures for the adsorbent were below unit, close to zero, confirming the favorable uptake of MB process. From Table 2, the value of $1/n$ decreased as increasing temperature with a range from 0.0253 to 0.0304, indicating a normal Langmuir isotherm (Fytianos et al., 2000).

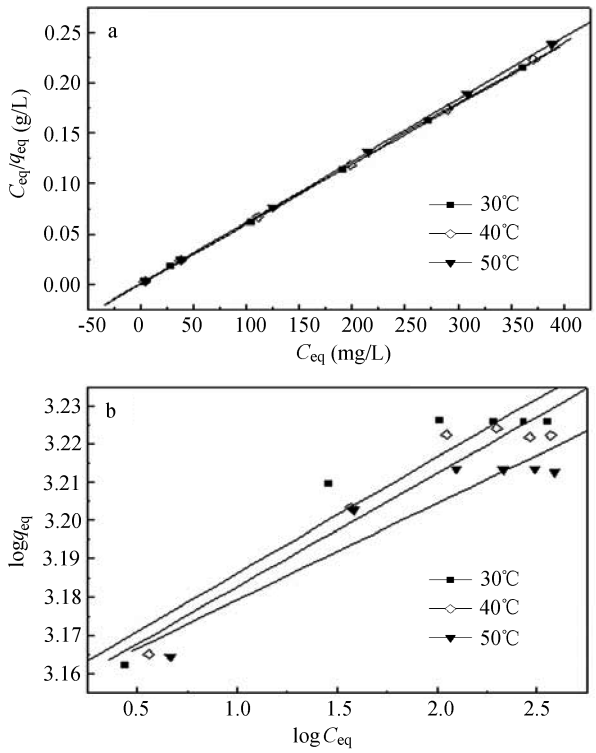

Fig. 9 Langmuir (a) and Freundlich (b) isotherms for MB onto adsorbent.

Table 2 Isotherm constants for MB on adsorbent CTS-*g*-PAA/10% VMT.

Model	Parameter			
Langmuir	T (°C)	30	40	50
	q_{eq} (mg/g)	1682.18	1675.59	1635.24
	q_m (mg/g)	1685.56	1672.85	1636.24
	$b\times10^{-5}$	6.36	5.19	7.37
	R^2	1	1	1
	$R_L\times10^4$	4.9	6.0	4.2
Freundlich	K_F ((mg/g)(L/mg)$^{1/n}$)	1431.43	1421.94	1425.28
	$1/n$	0.0304	0.0297	0.0253
	R^2	0.9094	0.9313	0.8865

2.10 Adsorption mechanism

In order to explain the adsorption mechanism of CTS-*g*-PAA/10% VMT hydrogel composite for MB, Fig. 10 represents the infrared spectra of CTS-*g*-PAA/10% VMT before and after MB adsorption of MB. It can be seen that the bands of MB at 1609, 1535, 1487 and 1443 cm^{-1} assigned to C–C of aromatic cycle stretching, were shifted and reduced after MB adsorption. The characteristic absorption bands of aromatic skeletal groups at 881, 830 and 793 cm^{-1} were broadened and reduced after adsorption. The band at 1724 cm^{-1} corresponding to –C═O stretching of –COOH was shifted and strengthened, and the bands at 1572 cm^{-1} and 1406 cm^{-1} ascribed to –COO$^-$ asymmetric stretching and –COO$^-$ symmetric stretching were shifted after adsorption. The bands at 1078 cm^{-1} and 1047 cm^{-1} ascribed to Si–O stretching, were shifted and reduced after adsorption (Tomanec et al., 1997). All the information indicated that the electrostatic attraction between –COO$^-$ groups and MB can describe the main adsorption process.

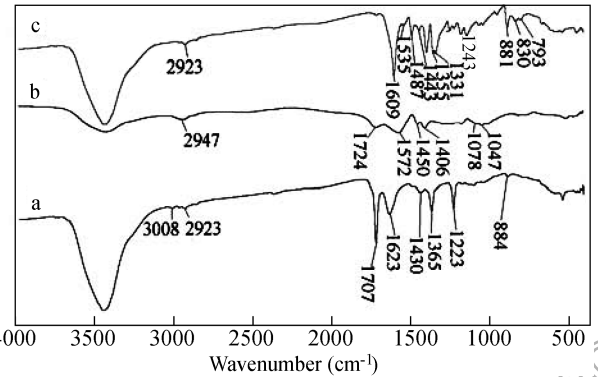

Fig. 10 Infrared spectra of MB loaded CTS-*g*-PAA/10% VMT (a), CTS-*g*-PAA/10% VMT (b) and MB (c).

3 Conclusions

In this study, a series of the hydrogel composites consisted of CTS, VMT and AA were prepared. FT-IR analysis suggests that during the copolymerization, PAA has grafted onto the backbone of CTS and VMT particles are successfully embedded within the polymeric networks. The results from batch experiments for the removal of MB show that the amount of dye uptake increases with increase in pH, contact time and initial concentration but decreases with the increase in temperature, ionic strength and SDS concentration in the present of SDS. The electrostatic attraction between $–COO^-$ groups and MB can describe the main adsorption process by FT-IR spectra before and after adsorption of MB on the hydrogel composite.

Acknowledgments

This work was supported by the National Natural Science Foundation of China (No. 20877077), and the Project of Jiangsu Provincial Science and Technology Office (No. BE2008087).

References

Aguedach A, Brosillon S, Morvan J, Lhadi E K, 2008. Influence of ionic strength in the adsorption and during photocatalysis of Reactive Black 5 azo dye on TiO_2 coated on non woven paper with SiO_2 as a binder. *Journal of Hazardous Materials*, 150(2): 250–256.

Barhoumi M, Beurroies I, Denoyel R, Saïd H, Hanna K, 2003. Coadsorption of phenol and nonionic surfactants onto clays. *Colloids and Surfaces A: Physicochemical and Engineering Aspects*, 223(1-3): 63–72.

Bhattacharyya K G, Sharma A, 2005. Kinetics and thermodynamics of Methylene Blue adsorption on Neem (*Azadirachta indica*) leaf powder. *Dyes and Pigments*, 65(1): 51–59.

Bukallah S B, Rauf M A, AlAli S S, 2007. Removal of Methylene Blue from aqueous solution by adsorption on sand. *Dyes and Pigments*, 74(1): 85–87.

Bulut E, Özacar M, Şengil Í A, 2008. Adsorption of malachite green onto bentonite: Equilibrium and kinetic studies and process design. *Microporous and Mesoporous Materials*, 115(3): 234–246.

Bulut Y, Aydın H, 2006. A kinetics and thermodynamics study of Methylene Blue adsorption on wheat shells. *Desalination*, 194(1-3): 259–267.

Cengiz S, Cavas L, 2008. Removal of Methylene Blue by invasive marine seaweed: *Caulerpa racemosa* var. *cylindracea*. *Bioresource Technology*, 99(7): 2357–2363.

Crini G, Badot P M, 2008. Application of chitosan, a natural aminopolysaccharide, for dye removal from aqueous solutions by adsorption processes using batch studies: A review of recent literature. *Progress in Polymer Science*, 33(4): 399–447.

Doğan M, Alkan M, Türkyilmaz A, Özdemir Y, 2004. Kinetics and mechanism of removal of Methylene Blue by adsorption onto perlite. *Journal of Hazardous Materials B*, 109(1-3): 141–148.

Eren E, Afsin B, 2007. Investigation of a basic dye adsorption from aqueous solution onto raw and pre-treated sepiolite surfaces. *Dyes and Pigments*, 73(2): 162–167.

Fytianos K, Voudrias E, Kokkalis E, 2000. Sorption-desorption behavior of 2,4-dichlorophenol by marine sediments. *Chemosphere*, 40(1): 3–6.

Ghasemi J, Asadpour S, 2007. Thermodynamics' study of the adsorption process of Methylene Blue on activated carbon at different ionic strengths. *Journal of Chemical Thermodynamics*, 39(6): 967–971.

Haghseresht F, Lu G Q, 1998. Adsorption characteristics of phenolic compounds onto coal-reject-derived adsorbents. *Energy Fuels*, 12(6): 1100–1107.

Hall K R, Eagleton L C, Acrivos A, Vermeulen T, 1966. Pore- and solid-diffusion kinetics in fixed-bed adsorption under constant-pattern conditions. *Industrial and Engineering Chemistry Fundamentals*, 5(2): 212–223.

Hameed B H, 2009. Spent tea leaves: A new non-conventional and low-cost adsorbent for removal of basic dye from aqueous solutions. *Journal of Hazardous Materials*, 161(2-3): 753–759.

Ho Y S, McKay G, 1998. Sorption of dye from aqueous solution by peat. *Chemical Engineering Journal*, 70(2): 115–124.

Janoš P, Buchtová H, Rýznarová M, 2003. Sorption of dyes from aqueous solution onto fly ash. *Water Research*, 37(20): 4938–4944.

Janoš P, Šmídová V, 2005. Effects of surfactants on the adsorptive removal of basic dyes from water using an organomineral sorbent–iron humate. *Journal of Colloid and Interface Science*, 291(1): 19–27.

Kannan N, Sundaram M M, 2001. Kinetics and mechanism of removal of Methylene Blue by adsorption on various carbons – a comparative study. *Dyes and Pigments*, 51(1): 25–40.

Lagergren S, Svenska B K, 1898. Zur theorie der sogenannten adsorption geloester stoffe. *Vetenskapsakad Handlingar*, 24(4): 1–39.

Lee W F, Yang L G, 2004. Superabsorbent polymeric materials. XII. Effect of montmorillonite on water absorbency for poly (sodium acrylate) and montmorillonite nanocomposite superabsorbents. *Journal of Applied Polymer Science*, 92(5): 3422–3429.

Li A, Wang A Q, Chen J M, 2004. Studies on poly (acrylic acid)/attapulgite superabsorbent composite. I. Synthesis and characterization. *Journal of Applied Polymer Science*, 92(3): 1596–1603.

Lin J M, Wu J H, Yang Z F, Pu M L, 2001. Synthesis and properties of poly (acrylic acid)/mica superabsorbent nanocomposite. *Macromolecular Rapid Communications*, 22(6): 422–424.

Meshko V, Markovska L, Mincheva M, Rodrigues A E, 2001. Adsorption of basic dyes on granular acivated carbon and natural zeolite. *Water Research*, 35(14): 3357–3366.

Nandi B K, Goswami A, Purkait M K, 2009. Adsorption characteristics of brilliant green dye on kaolin. *Journal of Hazardous Materials*, 161(1): 387–395.

Özcan A S, Özcan A, 2004. Adsorption of acid dyes from aqueous solutions onto acid-activated bentonite. *Journal of Colloid and Interface Science*, 276(1): 39–46.

Özer A, Dursun G, 2007. Removal of Methylene Blue from aqueous solution by dehydrated wheat bran carbon. *Journal of Hazardous Materials*, 146(1-2): 262–269.

Paulino A T, Guilherme M R, Reis A V, Campese G M, Muniz E C, Nozaki J, 2006. Removal of Methylene Blue dye from an aqueous media using superabsorbent hydrogel supported on modified polysaccharide. *Journal of Colloid and Interface Science*, 301(1): 55–62.

Qada E N E, Allen S J, Walker G M, 2006. Adsorption of

Methylene Blue onto activated carbon produced from steam activated bituminous coal: A study of equilibrium adsorption isotherm. *Chemical Engineering Journal*, 124(1-3): 103–110.

Qodah Z A, 2000. Adsorption of dyes using shale oil ash. *Water Research*, 34(17): 4295–4303.

Qu B C, Zhou J T, Xiang X M, Zheng C L, Zhao H X, Zhou X B, 2008. Adsorption behavior of Azo Dye C. I. Acid Red 14 in aqueous solution on surface soils. *Journal of Environmental Sciences*, 20(6): 704–709.

Robinson T, McMullan G, Marchant R, Nigam P, 2001. Remediation of dyes in textile effluent: A critical review on current treatment technologies with a proposed alternative. *Bioresource Technology*, 77(3): 247–255.

Sanghi R, Bhattacharya B, 2002. Review on decolorisation of aqueous dye solutions by low cost adsorbents. *Coloration Technology*, 118(5): 256–269.

Senthilkumaar S, Varadarajan P R, Porkodi K, Subbhuraam C V, 2005. Adsorption of methylene blue onto jute fiber carbon: Kinetics and equilibrium studies. *Journal of Colloid and Interface Science*, 284(1): 78–82.

Tan I A W, Ahmad A L, Hameed B H, 2008. Adsorption of basic dye on high-surface-area activated carbon prepared from coconut husk: Equilibrium, kinetic and thermodynamic studies. *Journal of Hazardous Materials*, 154(1-3): 337–346.

Tomanec R, Popov S, Vučinič D, Lazič P, 1997. Vermiculite from Kopaonik (Yugoslavia) characterization and processing. *Fizykochem Problemy Mineral*, 31: 247–254.

Wang L, Wang A Q, 2007. Adsorption characteristics of Congo Red onto the chitosan/montmorillonite nanocomposite. *Journal of Hazardous Materials*, 147(3): 979–985.

Wang L, Zhang J P, Wang A Q, 2008a. Removal of methylene blue from aqueous solution using chitosan-*g*-poly (acrylic acid)/montmorillonite superadsorbent nanocomposite. *Colloids and Surfaces A: Physicochemical and Engineering Aspects*, 322(1-3): 47–53.

Wang P, Fan X R, Cui L, Wang Q, Zhou A H, 2008b. Decolorization of reactive dyes by laccase immobilized in alginate/gelatin blent with PEG. *Journal of Environmental Sciences*, 20(12): 1519–1522.

Weber W J, Morris J C, 1962. Proceedings of the International Conference on Water Pollution Symposium. Oxford, Pergamon. 231–266.

Weng C H, Pan Y F, 2006. Adsorption characteristics of Methylene Blue from aqueous solution by sludge ash. *Colloids and Surfaces A: Physicochemical and Engineering Aspects*, 274(1-3): 154–162.

Xie Y T, Wang A Q, 2009. Study on superabsorbent composites XIX. Synthesis, characterization and performance of chitosan-*g*-poly (acrylic acid)/vermiculite superabsorbent composites. *Journal of Polymer Research*, 16(2): 143–150.

Zhao M F, Tang Z B, Liu P, 2008. Removal of Methylene Blue from aqueous solution with silica nano-sheets derived from vermiculite. *Journal of Hazardous Materials*, 158(1): 43–51.